Genetic Dissection of Interaction between Poliovirus 3D Polymerase and Viral Protein 3AB

DEBRA A. HOPE, SCOTT E. DIAMOND,† AND KARLA KIRKEGAARD*

*Department of Molecular, Cellular and Developmental Biology and Howard Hughes Medical Institute,
University of Colorado, Boulder, Colorado 80309*

Poliovirus RNA-dependent RNA polymerase 3D and viral protein 3AB are both thought to be required for the initiation of RNA synthesis. These two proteins physically associate with each other and with viral RNA replication complexes found on virus-induced membranes in infected cells. An understanding of the interface between 3D and 3AB would provide a first step in visualizing the architecture of the multiprotein complex that is assembled during poliovirus infection to replicate and package the viral RNA genome. The identification of mutations in 3D that diminish 3D-3AB interactions without affecting other functions of 3D polymerase is needed to study the function of the 3D-3AB interaction in infected cells. We describe the use of the yeast two-hybrid system to isolate and characterize mutations in 3D polymerase that cause it to interact less efficiently with 3AB than wild-type polymerase. One mutation, a substitution of leucine for valine at position 391 (V391L), resulted in a 3AB-specific interaction defect in the two-hybrid system, causing a reduction in the interaction of 3D polymerase with 3AB but not with another viral protein or a host protein tested. In vitro, purified 3D-V391L polymerase bound to membrane-associated 3AB with reduced affinity. Poliovirus that contained the 3D-V391L mutation was temperature sensitive, displaying a pronounced conditional defect in RNA synthesis. We conclude that interaction between 3AB and 3D or 3D-containing polypeptides plays a role in RNA synthesis during poliovirus infection.

Poliovirus, a positive-strand RNA virus, is capable of infecting susceptible cells and directing the synthesis of at least 10,000 progeny RNA molecules in less than 6 h at 37°C. This feat takes place in the cytoplasm of cells that do not synthesize RNA from RNA templates in the absence of viral infection. RNA replication complexes form on membranous vesicles that contain viral proteins, newly synthesized viral RNA, and host proteins. Both RNA synthesis and RNA packaging occur in association with the membrane-associated replication complex (4, 22). However, neither the details of the assembly of the replication complex nor the roles of the individual virus and host components are well understood.

RNA-dependent RNA polymerase activity is provided by the viral polymerase, 3D. In vitro, purified 3D polymerase is dependent on an RNA template and either an RNA or DNA primer. The mechanism of priming in infected cells and the mechanism of the specificity exhibited for poliovirus RNA remain unknown. Although 3D polymerase is a soluble protein, a subpopulation of 3D molecules is associated with membranous replication complexes in infected cells (5, 30) and in extracts that support poliovirus replication (2). This suggests that the association is indirect, presumably mediated by protein-protein interactions.

A likely candidate for the membrane tether for 3D polymerase is viral protein 3AB, which associates with intracellular membranes in isolation (7, 32) and binds directly to polymerase 3D. Detergent-solubilized and purified 3AB can be coimmunoprecipitated with either 3D polymerase or 3CD protease

(18), which contains all 3D sequences but does not exhibit polymerase activity. Detergent-solubilized 3AB has been shown to stimulate both the polymerase activity of purified 3D polymerase (14, 21, 23) and the proteolytic activity of 3CD (14) in cell extracts. However, detergent-solubilized 3AB is not a substrate for 3CD cleavage, whereas membrane-associated 3AB is (18). Thus, a fully native conformation for 3AB has not yet been achieved by current purification schemes. In infected cells, protein 3AB is likely to be the direct precursor of 3B, also known as VPg, which is covalently attached to the 5′ ends of all newly synthesized poliovirus RNA molecules. It is possible that the association of 3AB with 3D could position 3B either to act as a primer for RNA synthesis (for a review, see reference 27). Learning the biochemical details of the interaction between 3D and 3AB may contribute to our understanding of the mechanism for priming of RNA synthesis as well as the assembly of RNA replication complexes in infected cells.

Are 3D-3AB interactions important for the viral replicative cycle, and, if so, at which step? In an attempt to identify alleles of 3D polymerase that are defective only in their interaction with 3AB, we have employed the yeast two-hybrid system, which is in wide use as a screen to identify proteins that interact with a protein of interest (10, 12). Here we describe the use of the two-hybrid system to demonstrate interactions between 3D polymerase and protein 3AB as fusion proteins in the yeast nucleus and to identify 3AB interaction-defective alleles of 3D polymerase. Several 3D alleles that affected interaction with 3AB were identified. All such mutations conferred temperature-sensitive growth phenotypes to polioviruses that contained them. One of the 3D alleles was found to contain a mutation, in which leucine was substituted for valine at position 391 (V391L), which conferred a defect in interaction with 3AB and not with any other protein with which 3D polymerase is known to interact in the two-hybrid system. This mutant polymerase, 3D-V391L, was purified and shown to bind less efficiently to membrane-associated 3AB than did the wild-type

---

* Corresponding author. Present address: Department of Microbiology and Immunology, Stanford University School of Medicine, Stanford, CA 94305. Phone: (650) 498-7075. Fax: (650) 498-7185. E-mail: karlak@leland.stanford.edu.

† Present address: Departments of Medicine and Biochemistry, Biophysics and Genetics, University of Colorado Health Sciences Center, Denver, CO 80262.

polymerase, providing an independent confirmation that this mutant polymerase displays reduced affinity for 3AB. Thus, Val-391 is likely to be found on the surface of 3D polymerase that directly contacts the 3AB protein. The conditional defects of virus that contained the V391L mutation were consistent with a role for 3D-3AB interactions in viral RNA synthesis.

MATERIALS AND METHODS

Strains and plasmids. *Saccharomyces cerevisiae* EGY40 (*MATα his3 trp1 ura3-52 leu2*) was the recipient strain for all two-hybrid experiments described herein (11). Plasmid transformations were performed by the lithium acetate-polyethylene glycol method of either Elble (9) or Schiestl and Geitz (29). Yeast strains were routinely grown in synthetic medium lacking uracil, histidine, and tryptophan to select for the reporter, bait, and prey plasmids (see below), respectively. Liquid and solid media contained 2% glucose for normal growth. For liquid β-galactosidase assays, 2% raffinose was used to relieve glucose repression before induction of prey hybrid expression with 2% galactose (1). To observe colony color differences in plate assays, X-Gal (5-bromo-4-chloro-3-indolyl-β-D-galactopyranoside) was added to cooled buffered media containing 2% galactose at 40 μg/liter (1).

All plasmids and strains used in the two-hybrid system and interaction trap studies were generous gifts of Roger Brent (Harvard Medical School). All plasmids contain the yeast plasmid 2μm origin of replication. The reporter plasmid pSH18-34 (12) contains eight LexA operators upstream of the *Escherichia coli lacZ* gene. Strains that contain only this URA3-bearing plasmid do not produce detectable β-galactosidase activity (12).

The plasmid pLex202+PL contains the HIS3 marker and the entire coding sequence of the *E. coli* DNA binding protein LexA, which is the N terminus of all bait hybrid constructs. pRFHM1, used as a negative-control bait plasmid, expresses a fusion protein (LexBicoid) consisting of LexA and the *Drosophila* protein Bicoid (12). The plasmid that encodes Lex3D (pLex3D) expresses the 202 amino acids of LexA fused in frame with the 461-amino-acid coding sequence of poliovirus polymerase 3D (13, 24) with the additional residues Glu, Phe, and Met between the LexA and 3D coding sequences. To construct pLex3D, wild-type 3D sequences were amplified by PCR with primers AGTCAAGAAA TCATGGTGAAATCCAGTGG and TCGACTCTCGAGGTAGGGTTACTA AAATGAGTC. The PCR products obtained contained poliovirus nucleotides 5987 to 7384 flanked by *Eco*RI and *Xho*I restriction sites. The resulting *Eco*RI-*Xho*I fragment was cloned into the *Eco*RI and *Sal*I sites of pLex202+PL.

The plasmid pJG4-5 encodes the TRP1 marker and is the parent plasmid for the prey constructs. Under the control of the galactose-dependent GAL1 promoter, it encodes the B42 transcriptional activation domain from *E. coli* that functions in *S. cerevisiae* (15), the simian virus 40 T-antigen nuclear localization signal, and the hemagglutinin epitope tag (12). These sequences are abbreviated as B42 and are the N termini of all prey fusions. Prey plasmid B42-3AB encodes B42 fused to the 109 amino acids of poliovirus protein 3AB. 3AB sequences were amplified with primers TTTCAAGAATTCATGGGACCACTCCAGTAT and TGGTCCCTCGAGTTATTGTACCTTTGCTGTT, resulting in PCR products that contained poliovirus nucleotides 5111 to 5437 with flanking *Eco*RI and *Xho*I restriction sites to facilitate cloning into the *Eco*RI and *Xho*I sites of the prey plasmid pJG4-5. The plasmid that encodes the fusion protein B42-3D was prepared by inserting the *Eco*RI-*Xho*I fragment resulting from the PCR amplification of 3D polymerase sequences (see bait constructs above) into pJG4-5. The plasmid encoding B42-Sam68 (B42 fused to the 191 C-terminal amino acids of human protein Sam68) was a gift from Anne McBride (Stanford University) (16). The portions of each clone that were derived by PCR were sequenced to confirm that wild-type sequences were obtained.

Mutagenesis of the Lex3D bait plasmid. The Lex3D plasmid was mutagenized with hydroxylamine as described by Busby et al. (6) with some modifications. After mutagenesis, hydroxylamine was removed and replaced with a solution containing 10 mM Tris (pH 8.0) and 1 mM EDTA by using a Centricon-100 centrifugal concentrator column according to the instructions of the manufacturer (Amicon). Strain EGY40, which contained both the B42-3AB prey and the pSH18-34 reporter plasmids, was transformed with the mutagenized 3D bait plasmids. A collection of 5,000 His$^+$ yeast strains was selected at 30°C. Each colony was tested for β-galactosidase production in the presence of galactose by replica plating onto X-Gal indicator plates followed by incubation at 25 or 37°C. The colony color of the mutants was compared to that of an EGY40(pSH18-34, pLex3D, pB42-3AB) control strain grown at the same temperature. Colonies which showed a more pronounced decrease in color at one temperature than at the other were selected for further study. Mutant Lex3D bait plasmids from such colonies were isolated by preparation of yeast extracts and transformation into *E. coli* (1). Plasmids prepared from *E. coli* were used to retransform yeast strain EGY40(pSH18-34, pB42-3AB) to confirm that the interaction-defective phenotype was due to the mutations contained in the pLex3D bait plasmid.

The amounts of Lex3D fusion protein produced by expression of the mutant plasmids were tested by immunoblotting with an anti-LexA antiserum obtained from R. Brent (Harvard Medical School).

Sequence analysis. Dideoxy sequencing was performed by standard protocols (Sequenase; U.S. Biochemical) with the following primers: CCCATTGCTACA

TAAGGGTA, complementary to poliovirus positive-strand nucleotides 6338 to 6357; TGTGAAAAGCAGCATATAGG, complementary to positive-strand nucleotides 6565 to 6583; TTGTACAGGTGGTGTGAGTG, complementary to positive-strand nucleotides 6794 to 6813; GTTACATTCTCCCATGTGAC, complementary to positive-strand nucleotides 7082 to 7101; ACTCAGGATCA CGTTCGCTC, identical to positive-strand nucleotides 7214 to 7233; and AAA ATGAGTCAAGCCAACG, complementary to positive-strand nucleotides 7352 to 7369.

β-Galactosidase assays. The β-galactosidase activity of cells was measured by the permeabilized-cell assay of Miller (17). Miller units are calculated as follows: (optical density at 420 nm [OD$_{420}$] × 1,000)/[OD$_{600}$ × time [in minutes] × volume [in milliliters]). Reaction times were typically 5 min, using 100 μl of a cell culture with an OD$_{600}$ of between 0.5 and 1.5. Under these conditions, β-galactosidase activity was linear with respect to both the amount of input cell extract and the time of incubation (data not shown). The cells were harvested at times after galactose induction when the appearance of β-galactosidase activity in control cells was increasing linearly with time (data not shown). In addition, because the presence of glucose negatively regulates expression of the GAL1 promoter, cells were deprived of glucose before the addition of galactose.

Single colonies of the strains to be tested were grown overnight at 30°C in 2 ml of selective glucose-containing medium. Twenty-five-microliter aliquots of the resulting saturated cultures were used to inoculate 5-ml quantities of selective medium containing 2% raffinose, and the cells were grown to an OD$_{600}$ of 0.5 to 1.0 at 30°C. Cultures were split, galactose was added to 2%, and incubation was continued either for 7 or 8 h at 25°C or for 4 h at 37°C. Three individually transformed colonies of each strain of interest were analyzed. The β-galactosidase activity of cells was measured by the permeabilized-cell assay of Miller; measured activities were normalized for cell number and time (17). Data reported are the averages of values for three samples; standard deviations are indicated.

3D polymerase purification. The wild-type 3D polymerase expression plasmid pT5T3D was constructed by Thale Jarvis (Ribozyme Pharmaceuticals, Inc., Boulder, Colo.) and contains the entire 3D coding sequence preceded by an initiator methionine codon. 3D-V391L was subcloned into the wild-type plasmid pT5T3D by substituting a *Dra*III-*Eco*RI fragment from the Lex3D-V391L bait plasmid. The presence of the mutation in the plasmid was confirmed by the determination of an extra *Ase*I site at nucleotide 7157. Mutant and wild-type polymerases were expressed in *E. coli* BL21(DE3)(pLysS) cells. All buffers and solutions contained 2 mM dithiothreitol 0.1 mM EDTA, and 0.02% sodium azide in addition to the other compounds indicated. Wild-type and V391L mutant polymerases were purified in parallel as described elsewhere (20). Fractions were pooled, adjusted to 60% glycerol, and stored at −70°C.

Membrane-bound 3AB preparation. 3AB in bacterially derived membranes was the gift of S. Schultz (University of Colorado, Boulder). 3AB was expressed in *E. coli* BL21(DE3) by isopropyl-β-D-thiogalactopyranoside (IPTG) induction as described by Lama et al. (14). Total *E. coli* membranes, with or without 3AB, were isolated from an S10 supernatant by centrifugation at 100,000 × *g*. The resulting pellet was resuspended in buffer containing 100 mM NaCl and 50 mM Tris (pH 7.6). All membrane fractions were stored at 4°C.

3D-3AB binding assay. Increasing amounts of 3D polymerase were incubated with membranes with or without 3AB in binding buffer containing 500 mM NaCl, 25 mM Tris (pH 8.0), and 10 mM dithiothreitol. Reaction mixtures (total volume, 25 μl each) were incubated for 30 min at room temperature and centrifuged for 2 min at 13,000 × *g*. Pellets were recovered and washed in binding buffer. The resulting pellet was resuspended in Laemmli buffer and analyzed by sodium dodecyl sulfate-polyacrylamide gel electrophoresis (SDS-PAGE) on a 12.5% polyacrylamide gel. The gel was stained with Coomassie blue and air dried between cellophane sheets. The dried transparent gel was scanned (Agfa Argus II) into an Adobe Photoshop file, which was analyzed by using ImageQuant (Molecular Dynamics). Protein amounts were determined by comparison of Coomassie staining values to those of standard curves of purified mutant and wild-type polymerases. For both mutant and wild-type polymerases, the Coomassie staining densities of the standard curve were within the linear range of the scanner and each of the experimental values was within the limits of the standard curve.

Cells and viruses. The mutations identified in the two-hybrid screen were introduced into the poliovirus cDNA clone T7pGem polio (28). HeLa cells were transfected, using DEAE dextran, with RNAs synthesized in vitro by T7 RNA polymerase, with the mutant cDNAs being used as templates (19, 28, 33). Transfected cell monolayers were overlaid with Dulbecco's modified Eagle medium containing 10% calf serum and 1% agar. Plaques were allowed to develop for 72 h at 32.5°C or 48 h at 39.5°C. Wild-type and mutant 3D-V391L virus stocks were prepared from single plaques isolated at 32.5°C whose titers were also determined at that temperature. Plaque assays were performed as described previously (8).

Temperature shift experiments. To determine the effect of a shift to the nonpermissive temperature on the synthesis of viral proteins, subconfluent HeLa cell monolayers in 60-mm-diameter plates were infected with wild-type or mutant virus at a multiplicity of infection (MOI) of 50 PFU per cell. At 7.5 h postinfection at 32.5°C, cells were incubated with 5 μCi of [^{35}S]methionine (New England Nuclear) for 15 min at either 32.5 or 37.5°C. Cytoplasmic extracts were prepared (8), and equal volumes of supernatant were analyzed on SDS–12.5% polyacryl-

TABLE 1. β-Galactosidase activities of two-hybrid control strains grown at 25 and 37°C

Lex bait	B42-prey	β-galactosidase activity at[a]:	
		25°C	37°C
Lex3D	B42-3AB	2,500 ± 300	500 ± 200
LexBicoid	B42-3AB	10 ± 10	1 ± 10
Lex3D	B42-none	20 ± 20	0 ± 0

[a] Values are the average Miller units for three cultures ± standard deviations. No β-galactosidase activity was observed in the absence of galactose.

amide gels. To analyze the effect of incubation at the nonpermissive temperature on processing and stability of newly synthesized viral proteins, cells were infected at 32.5°C as described above. At 7 h postinfection, cells were incubated with 5 μCi of [³⁵S]methionine for 15 min at this permissive temperature and chased for either 90 min at 32.5°C or 60 min at 39.5°C. Equal volumes of cytoplasmic extracts were analyzed on SDS–12.5% polyacrylamide gels. A PhosphorImager (Molecular Dynamics) was used to visualize labeled proteins, and images were prepared by using Adobe Photoshop and Adobe Illustrator (Adobe Illustrations, Inc.).

To determine the effect of a temperature shift on positive-strand RNA synthesis, cells were infected as described above. At 4 h postinfection at 32.5°C, half the cells were shifted to 39.5°C, and they were subsequently harvested at various times. Total cytoplasmic RNA was isolated and then immobilized on nitrocellulose membrane by the use of a dot blot apparatus, and positive-strand poliovirus RNA was quantified by hybridization to a ³²P-labeled RNA probe that contained negative-strand nucleotides 6016 to 5601. The amount of hybridized RNA was determined by using a standard curve prepared by blotting known amounts of poliovirus RNA on the same nitrocellulose membrane.

RESULTS

3D and 3AB interact in the two-hybrid system. Since previous work suggested that a physical interaction between 3D and 3AB proteins occurred in vitro (18, 21, 23, 36), we tested whether these two proteins interact in the yeast two-hybrid system. In the system we used, kindly provided by R. Brent, an interaction between a bait hybrid protein, which contains the DNA-binding domain of bacterial repressor protein LexA, and a prey hybrid protein, which contains sequences that can activate transcription, reconstitutes a transcription factor sufficient to activate transcription from a plasmid-encoded reporter gene that is downstream of the recognition sequences for LexA (12). To detect an interaction between the bait and prey hybrid proteins, however, it is crucial that neither hybrid protein activates transcription of the reporter gene on its own. As can be seen in Table 1, the Lex3D bait fusion protein did not activate transcription of β-galactosidase when expressed with the B42 transcriptional activation domain alone, as had been previously reported (16). Similarly, the B42-3AB prey fusion protein did not activate transcription of the reporter gene either in isolation (data not shown) or in the presence of pRFHM1, which encodes a protein consisting of LexA fused to the *Drosophila* protein Bicoid (12) (Table 1). However, strains containing plasmids that expressed both the Lex3D bait protein and the B42-3AB prey fusion protein produced at least 100 times more β-galactosidase activity when grown at either 25 or 37°C (Table 1). This increase in β-galactosidase production was completely dependent on the presence of galactose in the growth medium (data not shown).

Screen for mutations in Lex3D that affect 3D-3AB interactions in the two-hybrid system. The yeast two-hybrid system was used to identify mutations in Lex3D that cause conditional 3AB interaction defects. An interaction-defective phenotype of interest was defined as a reduction in blue colony color in the presence of mutated Lex3D bait, B52-3AB prey, and a β-galactosidase reporter at either 25 or 37°C, but not at both temperatures. The conditional nature of the screen was im-

posed to ensure that the fusion proteins were capable of interacting under at least one set of conditions, with the hope that mutations that conferred such conditionally defective interactions would display conditional phenotypes when tested in the virus.

The yeast strain EGY40 containing the reporter and the B42-3AB prey plasmids was transformed with hydroxylamine-mutagenized Lex3D-encoding plasmids. Several thousand transformants were selected at 30°C, replica plated onto plates that contained galactose and X-Gal, and screened at 25 and 37°C for conditional color phenotypes. To ensure that apparent defects in the 3AB-3D interaction were caused by a mutation in the Lex3D-encoding plasmid, the Lex3D plasmids were recovered from each of the interaction-defective isolates and reintroduced into an EGY40 strain that contained the B42-3AB prey and reporter plasmids. As an additional screen, immunoblot analysis was used to confirm that the levels of Lex3D mutant fusion proteins were comparable to the amount of wild-type Lex3D fusion protein made at either temperature.

Isolated mutant 3D alleles contained more than one mutation. Six mutant Lex3D bait plasmids that were found to confer interaction-defective phenotypes were isolated and sequenced. The mutations and interaction phenotypes of these 3AB-interaction-defective 3D alleles are shown in Table 2. Also shown is a summary of the immunoblot data comparing the expression levels of the mutant bait hybrid proteins to that of the wild-type Lex3D bait fusion protein at each temperature.

The most promising candidates for 3D proteins that might display specific defects in their interaction with 3AB were isolates Lex3D-1.1, Lex3D-4.1, and Lex3D-7.1. As determined by immunoblot analysis, yeast strains that contained these plasmids expressed amounts of Lex3D bait fusion protein comparable to those expressed in strains that contained wild-type Lex3D (Table 2 and data not shown). Interestingly, each of these plasmids contained at least two mutations within the 3D coding sequence (Table 2). This either may have resulted from excessive mutagenesis during the original hydroxylamine treatment or may indicate a requirement for more than one mutation to observe an interaction-defective phenotype on plates. The amino acid change T367I appeared in both the 3D-1.1 and the 3D-7.1 plasmids. The same mutation occurred independently in these two plasmids since the mutant plasmids were derived from separately mutagenized pools.

Mutant isolates Lex3D-1.3 and Lex3D-3.1 encode stop codons at amino acids 120 and 134, respectively. The presence of truncated proteins of the size predicted by the locations of these stop codons was confirmed by immunoblot analysis, as summarized in Table 2. It is not clear why truncated proteins gave rise to an apparently conditional defect in 3AB interaction. The expression levels of these truncated alleles also differed widely from strain to strain, which is consistent with their variable interaction-defective phenotypes. Because these truncated proteins do not contain the active site of the enzyme, they would presumably lead to inviable virus, and thus they were not studied further. Isolate Lex3D-7.2 contained three amino acid changes and four silent nucleotide changes. Immunoblot analysis indicated that this isolate expressed a reduced amount of fusion protein compared to the wild type, with this effect being most pronounced at 37°C (data not shown). Because the temperature-sensitive interaction-defective phenotype of this isolate could simply be the result of the lower concentration of Lex3D fusion protein at the higher temperature, it was not studied further.

C-terminal mutations of Lex3D-1.1, Lex3D-4.1, and Lex3D-7.1 are sufficient to disrupt the interaction with 3AB. To test whether the mutations in the 3D sequences were sufficient for

TABLE 2. Results of two-hybrid screens for mutations in Lex3D that reduce 3AB interactions

Mutant bait isolate	Interaction phenotype[a]	Amino acid changes (nucleotide)	Translationally silent nucleotide change(s)	Protein expression level[b]
Lex3D-1.1	Temperature sensitive	T44I (C6117T) T367I (C7086T)	None	WT
Lex3D-1.3	Cold sensitive	Y120 stop (T6346A) V121I (G6347A)	G6904A	Variable; truncated protein
Lex3D-3.1	Slightly cold sensitive	Q134 stop (C6386T)	C6838T	Variable; truncated protein
Lex3D-4.1	Cold sensitive	A57T (G6155A) G64D (G6177A) V391L (G7157T)	None	WT
Lex3D-7.1	Temperature sensitive	E56K (G6152A) T279I (C6822T) T367I (C7086T)	None	WT
Lex3D-7.2	Slightly temperature sensitive	S87L (C6246T) T92I (C6261T) D381N (G7127A)	C6248T, C6253T C6256T, C6259T	Reduced, especially at 37°C

[a] Colonies that displayed a temperature-sensitive phenotype were less blue than colonies that contained wild-type Lex3D at 37°C. Cold-sensitive phenotypes were less blue than the wild type at 25°C.

[b] Immunoblot analysis was performed with antiserum produced against LexA. Amounts of Lex3D mutant fusion proteins were compared to a standard curve for Lex3D wild-type (WT) fusion protein grown at the same temperature.

the defective interaction with 3AB and to determine which mutations in 3D were responsible for the interaction-defective phenotypes observed for isolates Lex3D-1.1, Lex3D-4.1, and Lex3D-7.1, the mutations were introduced either in combination or separately into the Lex3D-encoding plasmid. For both Lex3D-7.1 and Lex3D-4.1, the two mutations closest to the N terminus were introduced together while the mutations closest to the C terminus were introduced separately.

To quantify the interaction-defective phenotypes of these isolates, β-galactosidase activities in permeabilized cells were measured. Figure 1 shows the relative β-galactosidase activities of the strains grown at 25 or 37°C after transfer to galactose-containing medium. As shown in Fig. 1A and B, the T367I mutation, found in both isolates Lex3D-1.1 and Lex3D-7.1, was sufficient to cause the temperature-sensitive interaction with 3AB observed in the original isolates. The mutation V391L, found in isolate Lex3D-4.1, was also sufficient to produce the decrease in 3D-3AB interaction seen in the original isolate (Fig. 1C); interestingly, no temperature dependence of the reduced interaction was seen in this quantitative β-galactosidase assay. It is clear that the more-C-terminal mutation in each of the isolates is sufficient to cause the observed 3AB interaction-defective phenotype. None of the more-N-terminal mutations gave rise to the diminished-interaction phenotype. In fact, Lex3D-E56K,T279I and Lex3D-A57T,G64D (Fig. 1B and C, respectively) gave rise to a slight increase in β-galactosidase activity and thus an apparent increased interaction with 3AB at 37°C.

The interaction-defective phenotype of V391L is specific for 3AB. Poliovirus 3D polymerase is known to associate physically with other 3D polymerase molecules, forming large multimers in solution and binding cooperatively to RNA (20). Not surprisingly, interaction between fusion proteins encoded by Lex3D bait and B42-3D prey plasmids was also observed in the two-hybrid system (Fig. 2). In addition, 3D polymerase has been found to interact with the human protein Sam68 in the two-hybrid system (16) (Fig. 2). Since our goal was to identify mutant 3D polymerases that were specifically defective in interaction with 3AB and not, for example, those that were misfolded and might therefore fail to interact with other proteins, we tested the effect of two C-terminal mutations, T367I and V391L, on the interaction of Lex3D with prey proteins that contained wild-type 3D or Sam68 sequences. As shown in
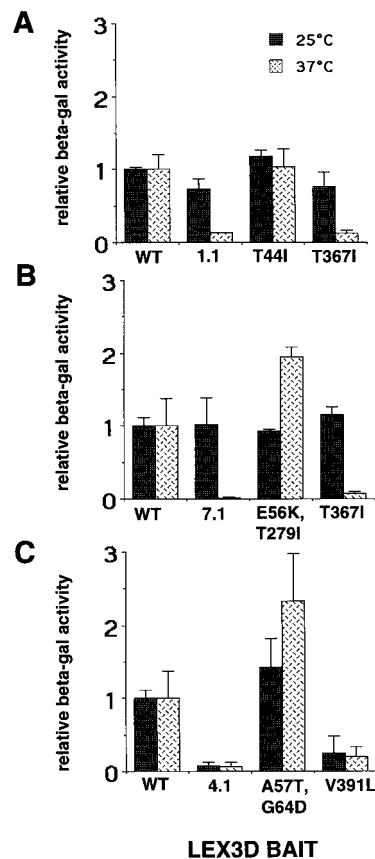

FIG. 1. Relative β-galactosidase (beta-gal) activity of Lex3D mutant bait fusion proteins with 3AB prey. Yeast cultures containing Lex3D mutants, B42-3AB prey, and a β-galactosidase reporter plasmid were split, induced with galactose, and incubated at either 25°C for 8 h or 37°C for 4 h. β-Galactosidase activity was measured by the permeabilized-cell assay of Miller (17). Values are the average numbers of Miller units for three different cultures ± the standard deviations for the samples. Miller units for Lex3D-WT with 3AB prey in this experiment were 2,500 ± 300 at 25°C and 500 ± 200 at 37°C. The activities of the mutants are expressed relative to the activity of the wild type (WT) at the same temperature. (A) Lex3D-1.1, Lex3D-T44I, and Lex3D-T367I; (B) Lex3D-7.1, Lex3D-E56K,T279I, and Lex3D-T367I; (C) Lex3D-4.1, Lex3D-A57T,G46D, and Lex3D-V391L.
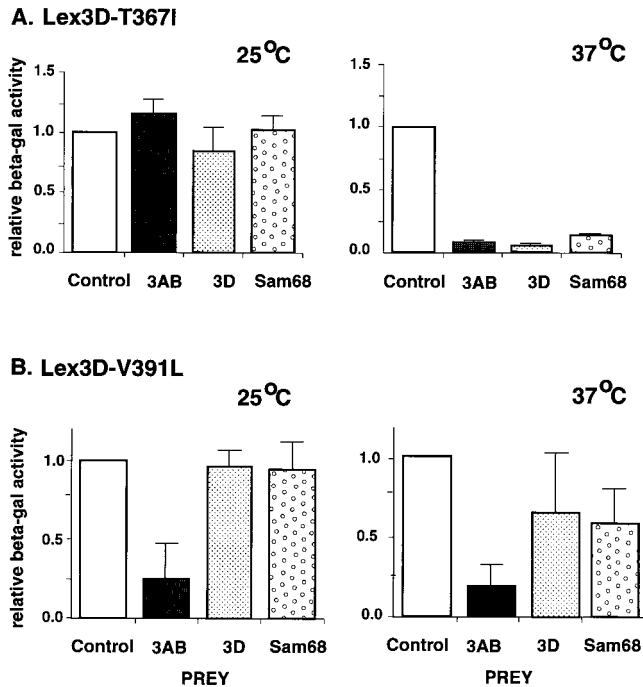
A. Lex3D-T367I

B. Lex3D-V391L

FIG. 2. Relative β-galactosidase (beta-gal) activities of Lex3D-T367I and Lex3D-V391L with 3AB, 3D, and Sam68 prey. β-Galactosidase activity was measured as described in the legend to Fig. 1. The activity of each mutant is expressed relative to the activity of the wild type at the same temperature and with the same prey. The ratio of wild-type polymerase to wild-type polymerase was, by definition, 1.0 for each bait used. However, experimental error in the wild-type measurements can be expressed as the error in relative Miller units following normalization. Relative Miller units ± standard deviation for the wild-type Lex3D bait–3AB prey control in this experiment were 1.0 ± 0.12 at 25°C and 1.0 ± 0.38 at 37°C. Relative Miller units for wild-type Lex3D bait–3D prey were 1.0 ± 0.03 at 25°C and 1.0 ± 0.15 at 37°C. Relative Miller units for wild-type Lex3D bait–Sam68 prey were 1.0 ± 0.15 at 25°C and 1.0 ± 0.14 at 37°C. (A) Signal for Lex3D-T367I bait normalized to that of wild-type 3D bait for 3AB, 3D, and Sam68 prey fusion proteins after growth at 25 and 37°C. (B) Signal for Lex3D-V391L bait normalized to that of wild-type 3D bait with 3AB, 3D, and Sam68 prey fusion proteins at 25 and 37°C.

Fig. 2A, Lex3D-T367I displayed reduced levels of reporter activity at 37°C with either B42-3D or B42-Sam68 prey proteins as well as with 3AB, indicating that the temperature-sensitive interaction phenotype observed between Lex3D-T367I and B42-3AB was not specific. However, Lex3D-V391L, which was nonconditionally defective in its interaction with B42-3AB prey, produced nearly as much reporter activity with either the B42-3D or the B42-Sam68 prey as did wild-type Lex3D at 25°C (Fig. 2B). Thus, the interaction-defective phenotype of Lex3D-V391L is specific for the 3D-3AB interaction at this temperature. Although this mutation results in reduced levels of interactions with B42-3D, B42-Sam68, and B42-3AB prey proteins at 37°C, the effect on B42-3AB interactions is the most severe (Fig. 2B). Because the V391L mutation specifically interferes with 3AB interactions, we suggest that this mutation identifies a region of 3D that interacts with 3AB.

The V391L mutation reduces the affinity of purified 3D polymerase for membrane-bound 3AB in vitro. To test whether the V391L mutation interfered with binding of 3D polymerase to 3AB directly, the affinities of purified mutant and wild-type polymerases for membrane-associated 3AB were measured. In accordance with a method devised by S. Schultz (30a), total membranes prepared from *E. coli* cells that do or do not express 3AB were incubated with increasing amounts of puri-

fied wild-type or 3D-V391L polymerase. The reaction mixtures were centrifuged, and the resulting pellets were washed and repelleted. The proteins contained in the pellets were analyzed by SDS-PAGE followed by Coomassie blue staining (Fig. 3). When either polymerase was incubated with *E. coli* membranes without 3AB, little polymerase was observed in the pellet (Fig. 3A and B). However, when 3AB was present in the membranes, larger amounts of 3D polymerase were recovered in the pellet fraction. At all concentrations tested, smaller amounts of 3D-V391L than wild-type polymerase were found in the membrane pellets (Fig. 3).

The amount of 3D polymerase bound to 3AB-containing membranes in this assay was quantified by scanning the Coomassie-stained gel and interpolating the number of pixels in each experimental band from standard curves of V391L mutant and wild-type polymerase (see Materials and Methods). Figure 3C shows the relationship between the amount of polymerase added and the amount of polymerase that bound to the
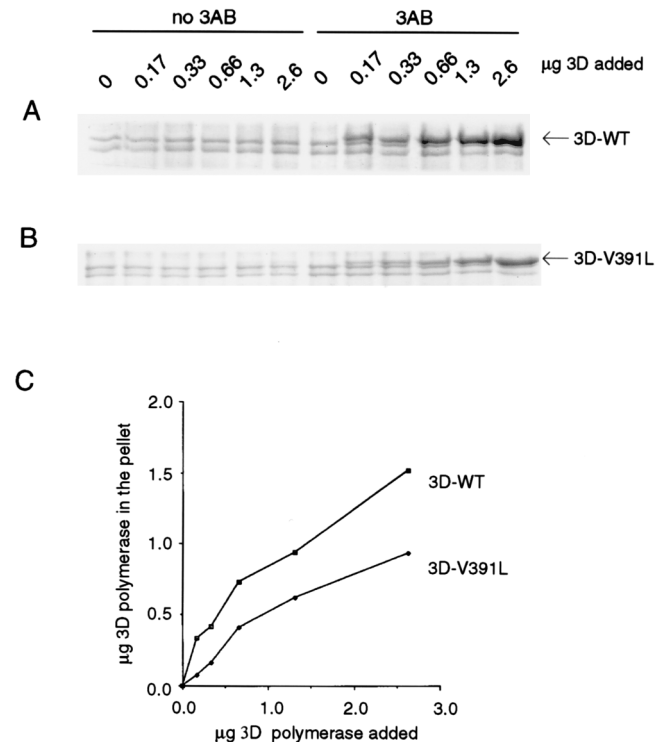

FIG. 3. Cosedimentation of wild-type (WT) and mutant 3D polymerase with *E. coli* membranes containing 3AB. Wild-type and mutant V391L 3D polymerases were individually incubated with *E. coli* membranes that did or did not contain 3AB; 3D polymerase migrates to just above the higher of two major *E. coli* proteins found in the membrane preparations. Also included on each gel was a titration of known amounts of purified wild-type or mutant polymerase, respectively. (A) Proteins in the pellets obtained after incubation of *E. coli* membranes that did or did not contain 3AB with increasing amounts of purified wild-type 3D polymerase. (B) Proteins in the pellets obtained after incubation of *E. coli* membranes that did or did not contain 3AB with increasing amounts of purified V391L mutant polymerase. (C) Quantitation of amount of 3D polymerase cosedimenting with *E. coli* membranes that contained 3AB as a function of polymerase concentration. Coomassie-stained gels were scanned with an Agfa Arcus II scanner to create .tif files. The Coomassie-stained polymerase bands were quantitated by using ImageQuant software (Molecular Dynamics). A standard curve relating arbitrary counts to densities of Coomassie staining of known amounts of polymerase was made for each gel. The standard curve was linearly responsive to the concentration of polymerase. The amount of polymerase in the pellet by virtue of interacting with 3AB was determined using the standard curve and subtracting the amount of 3D observed in the pellet in the absence of 3AB from that observed in the presence of 3AB.

3AB-containing membranes. The V391L mutant polymerase bound less efficiently to 3AB in membranes than the wild-type polymerase at all of the concentrations tested.

Phenotypes of viruses with mutations in 3D identified in the two-hybrid system. For 3D-V391L, diminished interaction with 3AB could be observed both in the yeast nucleus and in bacterially derived membranes that expressed 3AB. To test whether the V391L mutation or any of the other mutations in 3D that were found in the two-hybrid screen affected the replicative cycle of poliovirus, a variety of these amino acid substitutions were subcloned into a viral cDNA for analysis in tissue culture cells. This experiment was also intended to test whether two-hybrid interaction phenotypes can accurately predict viral phenotypes.

Transcripts that contained 3D-1.1, with both the T44I and T367I mutations, gave rise to a temperature-sensitive virus, as did those with either the T44I or T367I mutation in isolation (Fig. 4). Similarly, transcripts that contained 3D-7.1, with three mutations (Table 2), gave rise to a temperature-sensitive virus, as did those with both the E56K and T279I mutations or the T367I mutation in isolation (Fig. 4).

On the other hand, full-length poliovirus transcripts that contained 3D-4.1, with mutations A57T, G64D, and V391L, did not give rise to viable virus particles at any temperature. However, viruses that contained both the A57T and G64D mutations, as well as viruses that contained the single mutation V391L, were viable but temperature sensitive (Fig. 4). Since the V391L mutation caused an apparently specific defect in the interaction between 3D and 3AB, the 3D-V391L virus was further characterized to determine which step in the viral replicative cycle was defective at the nonpermissive condition.

3D-V391L virus synthesizes wild-type amounts of viral proteins at the nonpermissive temperature. To test whether the 3D-V391L temperature-sensitive virus displayed any defects in RNA translation, temperature shift experiments were performed. HeLa cells were infected with wild-type and 3D-V391L viruses at an MOI of 50 PFU per cell. After 7.5 h of incubation at 32.5°C, the permissive temperature for 3D-V391L, [^{35}S]methionine was added to the medium, and incubation was continued for 15 min at either 32.5 or 39.5°C. Two independent plaque isolates of 3D-V391L were shown to synthesize amounts of protein similar to those of the wild-type virus at either 32.5 or 39.5°C (Fig. 5). Therefore, this mutant did not display an obvious defect in translation after transfer to the nonpermissive temperature. In addition, no defects in the ability of the 3D-V391L virus to inhibit host cell translation were observed.

Addition of detergent-solubilized or membrane-associated 3AB to 3CD preparations is known to stimulate 3CD proteolytic activity (14, 18). We were curious to see if disruption of 3D-3AB interaction affected the processing of 3CD substrates. In the experiment shown in Fig. 5, the short (15-min) period of labeling with [^{35}S]methionine at both the permissive and nonpermissive temperatures was designed to detect any differences in translation. However, defects in protein processing should also be observable under these conditions; no differences between wild-type and V391L mutant virus in the ratios of precursors and products were observed (Fig. 5). To test whether 3D-V391L virus showed a defect in protein processing with longer periods of chase time at the nonpermissive temperature, infected cells were labeled with [^{35}S]methionine at the permissive temperature and chased with unlabeled methionine at either the permissive condition, 32.5°C, for 90 min or at the nonpermissive temperature, 39.5°C, for 60 min. Figure 6 shows the pattern of labeled proteins obtained. Note that the processing patterns are very comparable. Therefore, no significant
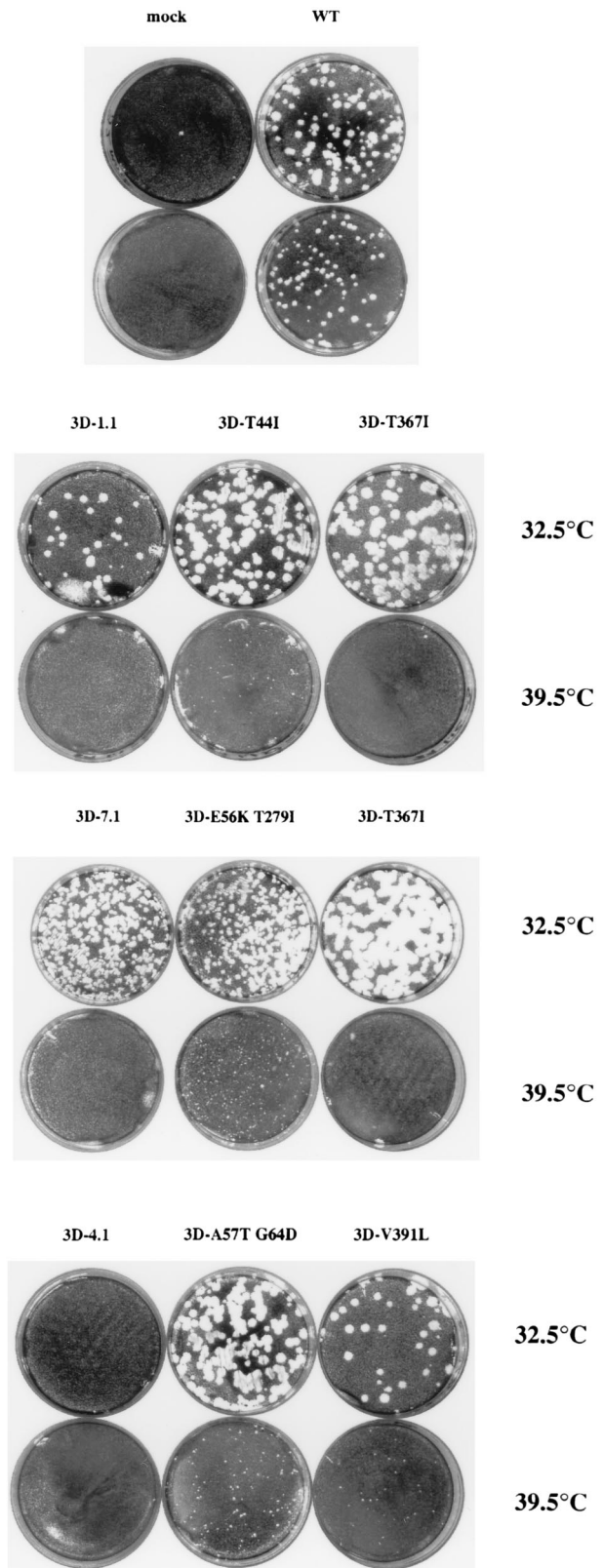

FIG. 4. Plaque phenotypes of polioviruses that contain mutations in 3D polymerase isolated in the two-hybrid screen. HeLa cells were infected with either wild-type virus or the mutant viruses indicated. Plaques were allowed to develop under agar for 72 h at 32.5°C or 48 h at 39.5°C. The dilutions of the mutant and wild-type strains are the same at each temperature. Mock, uninfected control; WT, wild-type poliovirus.
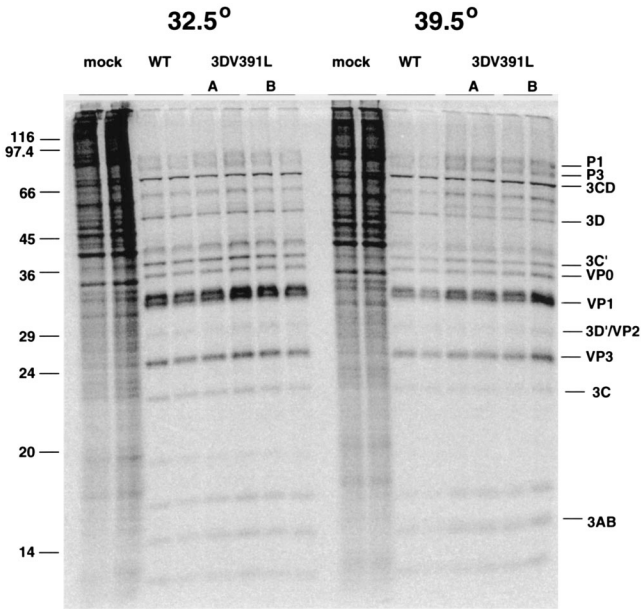
FIG. 5. [^{35}S]methionine-labeled virus proteins after translation at the permissive and nonpermissive temperatures. HeLa cells were infected in duplicate at an MOI of 50 PFU/cell with either wild-type (WT) or 3D-V391L virus and incubated at 32.5°C. At 7.5 h postinfection, [^{35}S]methionine was added, and the cells were then incubated for 15 min at either 32.5 or 39.5°C. Mock, no virus. Two plaque isolates of 3D-V391L (A and B) were used. Equal amounts of cytoplasmic extracts were analyzed by SDS-PAGE on a 12.5% polyacrylamide gel. Viral proteins are indicated to the right of the gel, and positions of molecular size markers (in kilodaltons) are shown on the left.

defect in protein processing is conferred by the V391L mutation.

3D-V391L virus is defective in RNA synthesis at the nonpermissive temperature. To test whether the 3D-V391L virus was defective for RNA synthesis, HeLa cells were infected with wild-type or 3D-V391L virus at an MOI of 50 PFU per cell. Cells were incubated for 4 h at the permissive temperature before being shifted to the nonpermissive temperature. Figure 7A shows that wild-type-virus-infected cells and cells infected with either of two independent isolates of 3D-V391L accumulated nearly identical levels of positive-strand RNA at the permissive temperature. In contrast, at the nonpermissive temperature of 39.5°C, cells infected with 3D-V391L virus accumulated two- to threefold less positive-strand RNA than cells infected with wild-type virus (Fig. 7B). Therefore, mutant 3D-V391L causes a temperature-sensitive RNA synthesis defect.

DISCUSSION

The two-hybrid system is well suited as a screen for mutations that disrupt protein-protein interactions. Phenotypic selection has been used by others to select for mutations in a protein of interest that exhibits decreased interaction with a binding partner in the two-hybrid system (31, 34, 35). Here, we have searched for conditional alleles in *S. cerevisiae* for which protein-protein interactions are disrupted under only one set of conditions, with the goal of isolating subtle mutations that might not abolish poliovirus growth when reintroduced into an infectious cDNA clone. If the protein of interest interacts with several prey fusion proteins, it is possible to screen for a loss of interaction that is specific for one prey and thus identify residues important for the interaction. Conversely, this screen could be used to identify residues important for the folding or

conformational stability of the fusion protein by screening for conditional, pleiotropic interaction defects.

The 3D mutant V391L displayed a specific interaction defect with 3AB at 25°C, suggesting that this residue has a role in the 3D-3AB interaction. Whether the effect of this mutation is direct or indirect remains to be determined. However, that bait fusion proteins which contain the V391L mutation are still capable of interacting with prey fusion proteins which contain either viral 3D or human Sam68 sequences at 25°C argues that the overall folding of the protein is not drastically perturbed under these conditions and is evidence of a direct interaction between V391 and 3AB protein. The T367I mutation, on the other hand, is likely to destabilize or alter the folding of 3D as a bait fusion protein, because it showed reduced interaction with all prey fusion proteins tested.

The more-N-terminal mutations, 3D-A57T,G64D and 3D-E56K,T279I, which may interact more efficiently with 3AB at a high temperature, gave rise to temperature-sensitive viruses. Since the two changes in these alleles have not been tested separately, we do not know which one is responsible for the virus phenotype. Richards et al. (25, 26) have recently identified two nucleotide binding sites in 3D polymerase, involving Lys-61 at one site and either Lys-276, Lys-278, or Lys-283 at the other. It is possible that the viral phenotypes, and even altered 3AB binding of these 3D alleles, could be related to altered nucleotide binding affinity.

Is the two-hybrid system a good predictor of viral phenotypes? For the originally isolated alleles that contained multiple mutations, the conditional interaction phenotypes in the yeast two-hybrid system corresponded to either conditional or lethal phenotypes in the virus. Although the individual contributions of some of the N-terminal mutations have not been determined, it is interesting to note that none of the mutations identified through use of the two-hybrid system gave rise to
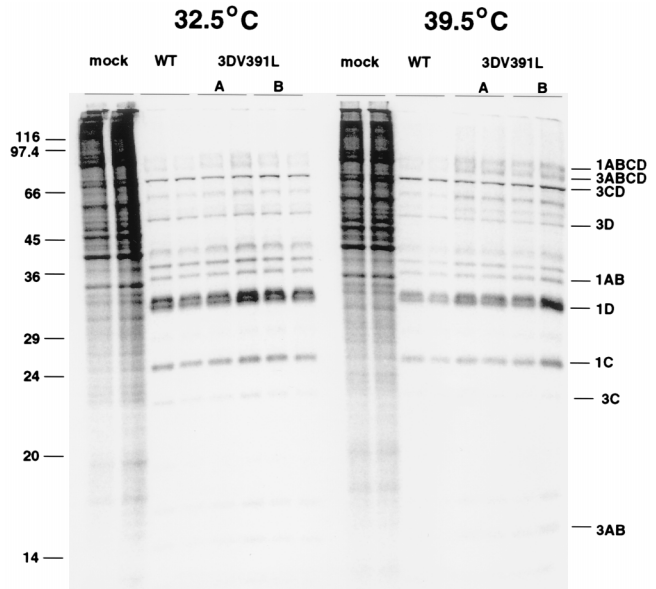

FIG. 6. Protein processing at the permissive and nonpermissive temperature for 3D-V391L virus. HeLa cells were infected as described in the legend to Fig. 5. At 7 h postinfection, cells were labeled with [^{35}S]methionine for 15 min at 32.5°C. The cells were then grown in non-radioactively labeled medium for 90 min at 32.5°C or 60 min at 39.5°C. Extracts were prepared and analyzed as described in the legend to Fig. 5. Viral proteins are indicated to the right of the gel, and the positions of molecular size markers (in kilodaltons) are shown on the left. WT, wild type.
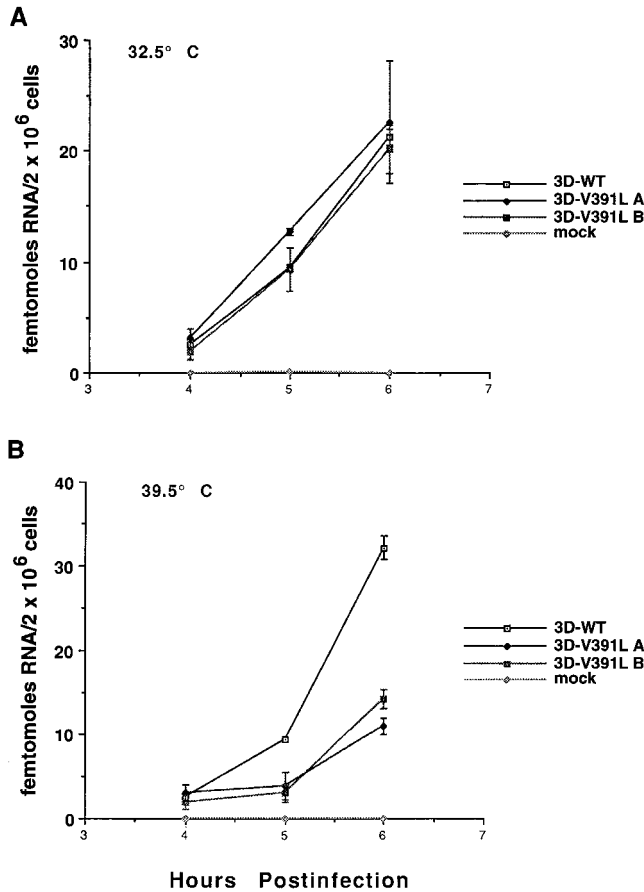
A

B

Hours Postinfection

FIG. 7. Accumulation of poliovirus positive-sense RNA in infected cells after temperature shift. HeLa cells were infected in duplicate at an MOI of 50 PFU/cell with either wild-type poliovirus or one of two independent isolates (A and B) of the mutant virus 3D-V391L. Cytoplasmic RNA was isolated from poliovirus-infected HeLa cells and analyzed by dot blotting. RNA was identified by using a poliovirus-specific probe that was complementary to the positive strand. The hybridized radioactivity was quantified with ImageQuant software and a PhosphorImager. The number of femtomoles of RNA in each sample of 10^6 cells was calculated by extrapolation from a curve of known amounts of poliovirus positive-sense RNA. (A) Cells were incubated at 32.5°C throughout the infection. (B) Cells were shifted to 39.5°C after 4 h of incubation at 32.5°C. mock, uninfected control.

wild-type virus. In fact, although some of the mutations (Fig. 1) conferred nonconditional defects to the 3D-3AB interaction in the two-hybrid system (3D-4.1 and 3D-V391L), caused no detectable defect in the 3D-3AB interaction (3D-T44I), or apparently increased the 3D-3AB interaction (3D-E56K,T279I and 3D-A57T,G64D), all but one of the viruses that contained these mutations were temperature sensitive (Fig. 3). Possible explanations for these mutant phenotypes include defects in viral RNA structure or function caused by the mutations and defects in protein folding or conformation for all mutant polymerases. However, the simplest explanation for this result is that the process(es) governed by 3D-3AB interactions during viral infection is more rate limiting at 39.5°C than at 32.5°C. In any case, whether the two-hybrid system assays 3AB-3D interactions per se or the folding or flexibility of the 3D molecule, the two-hybrid system results reflect some aspect of 3D polymerase structure or function that is also important to the virus.

We isolated one allele, 3D-V391L, that appeared to be specifically defective for interaction with 3AB in the two-hybrid system. Purified V391L polymerase showed a reduced affinity

for membrane-associated 3AB in vitro as well. Poliovirus that contained the V391L mutation displayed a pronounced defect in RNA synthesis upon a shift to the nonpermissive temperature. If the reduced interaction with 3AB were the only defect in V391L polymerase, we could conclude that the phenotypes of the V391L virus demonstrated that 3D-3AB interactions are crucial during viral infection. However, the possibility that effects of the 3D V391L mutation on 3CD protease activity, 3D polymerase activity, or interactions with as-yet-unidentified ligands in infected cells are responsible for causing or exacerbating these phenotypes remains. We have observed that V391L polymerase displays slightly reduced activity in RNA elongation assays in vitro (data not shown). However, since the putative 3AB binding site discussed here might overlap with the RNA binding site on 3D polymerase (8a), this result is difficult to interpret.

Recently, Barton et al. (3) have described a 3D polymerase mutation, M394T, that leads to temperature-sensitive initiation of RNA synthesis in vitro. Because a possible role of the 3D-3AB interaction is in initiation of RNA synthesis, the proximity of this mutation to the one we identified is intriguing. Studies involving mutation of residues near V391L to test the hypothesis that this residue identifies a region of 3D that is in direct contact with 3AB are in progress.

REFERENCES

1. **Ausubel, F. M., R. Brent, R. E. Kingston, D. D. Moore, J. G. Seidman, J. A. Smith, and K. Struhl (ed.).** 1990. Current protocols in molecular biology. Greene Publishing Associates and Wiley Interscience, New York, N.Y.
2. **Barton, D. J., E. P. Black, and J. B. Flanegan.** 1995. Complete replication of poliovirus in vitro: preinitiation RNA replication complexes require soluble cellular factors for the synthesis of VPg-linked RNA. J. Virol. **69:**5516–5527.
3. **Barton, D. J., B. J. Morasco, L. Eisner-Smerage, P. S. Collis, S. E. Diamond, M. J. Hewlett, M. A. Merchant, B. J. O'Donnell, and J. B. Flanegan.** 1996. Poliovirus RNA polymerase mutation 3D-M394T results in a temperature-sensitive defect in RNA synthesis. Virology **217:**459–469.
4. **Bienz, K., D. Egger, and L. Pasamontes.** 1987. Association of polioviral proteins of the P2 genomic region with the viral replication complex and virus-induced membrane synthesis as visualized by electron microscopic immunocytochemistry and autoradiography. Virology **160:**220–226.
5. **Bienz, K., D. Egger, Y. Rasser, and W. Bossart.** 1983. Intracellular distribution of poliovirus proteins and the induction of virus-specific cytoplasmic structures. Virology **131:**39–48.
6. **Busby, S., M. Irani, and B. de Crombrugghe.** 1982. Isolation of mutant promoters in the *Escherichia coli* galactose operon using local mutagenesis on cloned DNA fragments. J. Mol. Biol. **154:**197–209.
7. **Datta, U., and A. Dasgupta.** 1994. Expression and subcellular localization of poliovirus VPg-precursor protein 3AB in eukaryotic cells: evidence for glycosylation in vitro. J. Virol. **68:**4468–4477.
8. **Diamond, S. E., and K. Kirkegaard.** 1994. Clustered charged-to-alanine mutagenesis of poliovirus RNA-dependent RNA polymerase yields multiple temperature-sensitive mutants defective in RNA synthesis. J. Virol. **68:**863–876.
8a. **Ehrenfeld, E.** Personal communication.
9. **Elble, R.** 1992. A simple and efficient procedure for transformation of yeasts. BioFeedback **13:**18–20.
10. **Fields, S., and O. Song.** 1989. A novel genetic system to detect protein-protein interactions. Nature **340:**245–246.
11. **Golemis, E. A., and R. Brent.** 1992. Fused protein domains inhibit DNA binding by LexA. Mol. Cell. Biol. **12:**3006–3014.
12. **Gyuris, J., E. A. Golemis, H. Chertkov, and R. Brent.** 1993. Cdi1, a human G1 and S phase protein phosphatase that associates with Cdk2. Cell **75:**791–803.
13. **Kitamura, N., B. L. Semler, P. G. Rothberg, G. R. Larsen, C. J. Adler, A. J. Dorner, E. A. Emini, R. Hanecak, J. J. Lee, S. van der Werf, C. W. Anderson,**

and E. Wimmer. 1981. Primary structure, gene organization and polypeptide expression of poliovirus RNA. Nature **291:**547–553.

14. **Lama, J., A. V. Paul, K. S. Harris, and E. Wimmer.** 1994. Properties of purified recombinant poliovirus protein 3AB as substrate for viral proteinases and as co-factor for RNA polymerase 3D^{pol}. J. Biol. Chem. **269:**66–70.

15. **Ma, J., and M. Ptashne.** 1987. A new class of transcriptional activators. Cell **51:**113–119.

16. **McBride, A. E., A. Schlegel, and K. Kirkegaard.** 1996. Human protein Sam68 relocalization and interaction with poliovirus RNA polymerase in infected cells. Proc. Natl. Acad. Sci. USA **93:**2296–2301.

17. **Miller, J. H.** 1972. Experiments in molecular genetics. Cold Spring Harbor Laboratory, Cold Spring Harbor, N.Y.

18. **Molla, A., K. S. Harris, A. V. Paul, S. H. Shin, J. Mugavero, and E. Wimmer.** 1994. Stimulation of poliovirus proteinase 3Cpro-related proteolysis by the genome-linked protein VPg and its precursor 3AB. J. Biol. Chem. **269:**27015–27020.

19. **Novak, J. E., and K. Kirkegaard.** 1994. Coupling between genome translation and replication in an RNA virus. Genes Dev. **8:**1726–1737.

20. **Pata, J. D., S. C. Schultz, and K. Kirkegaard.** 1995. Functional oligomerization of poliovirus RNA-dependent RNA polymerase. RNA **1:**466–477.

21. **Paul, A. V., X. Cao, K. S. Harris, J. Lama, and E. Wimmer.** 1994. Studies with poliovirus polymerase 3D^{pol}. Stimulation of poly(U) synthesis in vitro by purified poliovirus protein 3AB. J. Biol. Chem. **269:**29173–29181.

22. **Pfister, T., D. Egger, and K. Bienz.** 1995. Poliovirus subviral particles associated with progeny RNA in the replication complex. J. Gen. Virol. **76:**63–71.

23. **Plotch, S. J., and O. Palant.** 1995. Poliovirus protein 3AB forms a complex with and stimulates the activity of the viral RNA polymerase, 3D^{pol}. J. Virol. **69:**7169–7179.

24. **Racaniello, V. R., and D. Baltimore.** 1981. Molecular cloning of poliovirus cDNA and determination of the complete nucleotide sequence of the viral genome. Proc. Natl. Acad. Sci. USA **78:**4887–4891.

25. **Richards, O. C., S. Baker, and E. Ehrenfeld.** 1996. Mutation of lysine residues in the nucleotide binding segments of the poliovirus RNA-dependent RNA polymerase. J. Virol. **70:**8564–8570.

26. **Richards, O. C., J. L. Hansen, S. Schultz, and E. Ehrenfeld.** 1995. Identification of nucleotide binding sites in the poliovirus RNA polymerase. Biochemistry **34:**6288–6295.

27. **Rueckert, R. R.** 1996. Picornaviridae and their replication, p. 609–654. *In* B. M. Fields, D. L. Knipe, and P. M. Howley (ed.), Virology. Lippincott-Raven, New York, N.Y.

28. **Sarnow, P.** 1989. Role of 3′-end sequences in infectivity of poliovirus transcripts made in vitro. J. Virol. **63:**467–470.

29. **Schiestl, R. H., and R. D. Geitz.** 1989. High efficiency transformation of intact yeast using single-stranded nucleic acids as a carrier. Curr. Genet. **16:**339–346.

30. **Schlegel, A., T. H. Giddings, Jr., M. S. Ladinsky, and K. Kirkegaard.** 1996. Cellular origin and ultrastructure of membranes induced during poliovirus infection. J. Virol. **70:**6576–6588.

30a.**Schultz, S.** Personal communication.

31. **Shih, H.-M., P. S. Goldman, A. J. DeMaggio, S. M. Hollenberg, R. H. Goodman, and M. F. Hoekstra.** 1996. A positive genetic selection for disrupting protein-protein interactions: identification of CREB mutations that prevent association with the coactivator CBP. Proc. Natl. Acad. Sci. USA **93:**13896–13901.

32. **Towner, J., and B. L. Semler.** 1996. Determinants of membrane association on poliovirus protein 3AB. J. Biol. Chem. **271:**26810–26818.

33. **van der Werf, S., J. Bradley, E. Wimmer, F. W. Studier, and J. J. Dunn.** 1986. Synthesis of infectious poliovirus RNA by purified T7 RNA polymerase. Proc. Natl. Acad. Sci. USA **83:**2330–2334.

34. **Vidal, M., R. K. Brachmann, A. Fattaey, E. Harlow, and J. D. Boeke.** 1996. Reverse two-hybrid and one-hybrid systems to detect dissociation of protein-protein and DNA-protein interactions. Proc. Natl. Acad. Sci. USA **93:**10315–10320.

35. **Vidal, M., P. Braun, E. Chen, J. D. Boeke, and E. Harlow.** 1996. Genetic characterization of a mammalian protein-protein interaction domain by using a yeast reverse two-hybrid system. Proc. Natl. Acad. Sci. USA **93:**10321–10326.

36. **Xiang, W., A. Cuconati, A. V. Paul, X. Cao, and E. Wimmer.** 1995. Molecular dissection of the multifunctional poliovirus RNA-binding protein 3AB. RNA **1:**892–904.